Conversion of Radiant Light Energy in Photobioreactors

J. F. Cornet, C. G. Dussap, and J. B. Gros
Lab. de Génie Chimique Biologique, Université Blaise Pascal, 63177 Aubiere Cedex, France

The conversion of radiant light energy into chemical affinity by microorganisms in photobioreactors is examined. The kinetics of entropy production in the system is theoretically established from entropy and energy balances for the material and photonic phases in the reactor. A negative chemical affinity term compensated for by a radiant energy term at a higher level of energy characterizes photosynthetic organisms. The local volumetric rate of radiant light energy absorbed, which appears in the dissipation function as an irreversible term, is calculated for monodimensional approximations providing analytical solutions and for general tridimensional equations requiring the solution of a new numerical algorithm. Solutions for the blue-green alga Spirulina platensis cultivated in photoreactors with different geometries and light energy inputs are compared. Thermodynamic efficiency of the photosynthesis is calculated. The highest value of 15% found for low radiant energy absorption rates corresponds to a maximum quantum yield in the reactor.

Introduction

When a photosynthetic microorganism is grown in a bioreactor, there are strong interactions between biological kinetics and availability of light energy in the vessel. This demands a quantitative understanding of light energy transport and use.

Basically, two kinds of problems must be simultaneously addressed:

- Conversion of light energy by microorganisms into heat and chemical potential; and
- Dispersion and absorption of light energy by radiative transfer throughout the liquid medium.

The process of photosynthesis involves conversion of light energy into chemical energy. The procedure is that photons are absorbed by a molecule (chlorophyll), expelling electrons via two photosystems towards an electron transport chain (ferredoxin) that acts as a redox system, which then produces high energy compounds (ATP and phosphorylated molecules) and hydrogen carriers such as NADPH, H^+ (Doelle, 1975).

In conversion of radiant energy into chemical energy, two coexisting phases have to be considered as suggested by Bird (1960) and Siegel and Howell (1992), the material phase consisting of all the mass in the system, and the photonic phase consisting of the electromagnetic radiation. This scheme implies solving three independent balance equations:

- Mass balance (Bird, 1960);
- Photonic phase balance knowing the expression of the local volumetric rate of radiant energy absorbed (Chandrasekhar, 1960; Spadoni et al., 1978; Aiba, 1982; Siegel and Howell, 1992); and
- Energy balance accounting for the interchanges of energy between the material phase and the photonic phase (Bird, 1960).

Additionally, an entropy balance can be obtained from the Gibbs equation, splitting the rate of entropy accumulation into a source term and a convective term (Prigogine, 1967; Glansdorff and Prigogine, 1971). This last balance affords the expression for the dissipation function, and a thermodynamic treatment of energy conversion which is of prime importance for biochemical reactions (Roels, 1983). The thermodynamics of irreversible processes is almost entirely concerned with the analysis of entropy production and the study of relations between rates and affinities. This analysis is necessary in order to ascertain which processes become possible through coupling, that is, using the entropy production of another process (Prigogine, 1967). This analysis implicitly includes thermodynamic efficiency and enthalpy efficiency for which the definitions for photobioconversions are still being debated (Aiba and Ogawa,

Correspondence concerning this article should be addressed to J. F. Cornet.

1977; Ogawa and Aiba, 1978; Ogawa et al., 1978; Lee and Pirt, 1982; Aiba and Ogawa, 1983; Lee et al., 1984; Iehana, 1987; Lee et al., 1987).

In a photobioreactor, the material phase can always be considered as homogeneous with respect to temperature and concentration, and isochoric. Conversely, radiant energy availability in an absorbing-emitting medium cannot generally be taken as identical throughout the vessel. In addition, in the case of photobioreactors, scattering of energy by solid particles such as suspended microorganisms is a source of added complexity. The energy distribution must be locally described to allow for the dispersion of light in all directions (Spadoni et al., 1978; Aiba, 1982).

Monodimensional geometries simplify the mathematical problem by reducing the information required to describe the projection of the photopropagation vectors along a single axis, which is then applicable to rectangular geometries (Cornet et al., 1992a). In the case of more complex geometries, the integro-differential and tridimensional form of the equation of radiative transfer must be solved numerically, generally by Monte-Carlo methods (Spadoni et al., 1978; Aiba, 1982).

This work describes how the four balances are established (mass balance, photonic phase balance, energy balance, and entropy balance) including local and integral expressions of the balances. This yields expressions for the dissipation function and the thermodynamic efficiency for photoconversions. An original finite-element method is proposed and used to discuss the results obtained both in batch and in continuous cultures for the growth of the cyanobacterium *Spirulina platensis* (blue-green algae) in a cylindrical (5 L), and two rectangular (1 L and 4 L) photoreactors.

Balance Equations

Mass and energy balances for the material phase

Local Mass Balance. The mass balance over an arbitrary differential fluid element is similar to the equation of continuity for each chemical species (Bird, 1960):

$$\frac{\partial C_i}{\partial t} = -\nabla \cdot N_i + r_i \tag{1}$$

where N_i stands for the molar flux with respect to fixed coordinates. The conversion of species i in the system results from several different chemical or biochemical reactions, each of them characterized by the stoichiometric coefficients ν_{ij}, such as r_i expressed by:

$$r_i = \sum_j \nu_{ij} J_j \tag{2}$$

J_j denoting the volumetric reaction rate of reaction j.

Local Internal Energy Balance. In the general case, for an open system the accumulation of internal energy is given by:

$$\frac{\partial u}{\partial t} = -P\nabla \cdot v - \nabla \cdot q + \eta\Phi - \nabla \cdot \int_0^\infty F_\lambda d\lambda - \nabla \cdot \sum_i N_i h_i \tag{3}$$

where N_i is a molar flux of i, h_i the molar enthalpy of i, F_λ the radiant energy flux for radiation of wavelength λ, and u is the internal energy per unit volume. Note that $\eta\Phi$ is the viscous dissipation function equal to $-(\tau:\nabla v)$, and that the Fourier law gives for the heat conduction flux $-\nabla \cdot q = \lambda_T \nabla^2 T$.

Importantly, the partial molar enthalpies of species h_i are not the enthalpies of the pure compounds, but the partial molar enthalpies of the compounds at their actual concentrations. Given solutions cannot generally be considered as ideal solutions; this applies both to the incoming and outgoing flows in the system.

The term $\nabla \cdot \int_0^\infty F_\lambda d\lambda$ represents the radiant energy transferred to the differential element of fluid. This term is calculated as the divergence of the radiant energy flux for wavelength λ and integrated over the entire spectrum. If emission is neglected, this term corresponds at steady state to the local volumetric rate of radiant energy absorbed $\mathfrak{A}$ (Bird, 1960):

$$\mathfrak{A} = -\nabla \cdot \int_0^\infty F_\lambda d\lambda \tag{4}$$

Note that the Eq. 3 leads, for example, to the determination of the tridimensional distribution of temperatures in a nonisothermal medium.

For the application of the above described equations to photobioreactors, the material phase can be considered as homogeneous and the reactor isochoric and isothermal. In this case, the integration of these balance equations is relatively straightforward.

Macroscopic Mass Balance. The spatial integration of Eq. 1 leads to:

$$\frac{dC_i}{dt} = \Phi_i + \frac{1}{V}\int_V r_i dV \tag{5}$$

The term $1/V \int_V r_i dV$ represents the overall transformation rate of component i, q_i:

$$q_i = \frac{1}{V}\int_V r_i dV \tag{6}$$

As the photobioreactor can be assumed to be perfectly mixed for each dissolved species, q_i is the only quantity experimentally observable. q_i can also be expressed using the kinetics of all the reactions in the system:

$$q_i = \frac{1}{V}\sum_j \nu_{ij} \int_V J_j dV \tag{7}$$

Macroscopic Internal Energy Balance. The spatial integration of Eq. 3 gives:

$$\frac{du}{dt} = \Phi_w + \Phi_q - \frac{1}{V}\int_V \nabla \cdot \int_0^\infty F_\lambda d\lambda\, dV + \sum_i \Phi_i h_i \tag{8}$$

The terms Φ_w and Φ_q represent the flows in the reactor associated with the mechanical work performed on the system

and with the heat exchange between the system and it surroundings. Therefore, Φ_w is the power supplied, and Φ_q the heat flow exchanged as defined by Glansdorff and Prigogine (1971).

Thus, under steady-state conditions, the following enthalpy balance is obtained:

$$\sum_i \Phi_i h_i = -\Phi_w - \Phi_q + \frac{1}{V}\int_V \nabla \cdot \int_0^\infty F_\lambda \, d\lambda \, dV \tag{9}$$

and Φ_q is then calculated by:

$$\Phi_q = -\Phi_w + \frac{1}{V}\int_V \nabla \cdot \int_0^\infty F_\lambda \, d\lambda \, dV - \sum_i \Phi_i h_i \tag{10}$$

The steady-state approximation (Eqs. 9 and 10) is valid for continuous processes; it can be extended to batch processes assuming the pseudo steady-state approximation, that is, neglecting the rate of accumulation of internal energy in order to estimate the heat exchanged. Nevertheless, Eq. 8 will be required for a rigorous derivation of energy balances.

There are four distinct contributions in the energy flow to a photobioreactor at steady state: a flow associated with heat Φ_q, one associated with the mechanical work performed on the system Φ_w, a flow associated with chemical substances, and one with the light energy input.

Entropy balance for the material phase

The second law of thermodynamics states that the change in entropy of an isolated system is positive. In order to determine the rate of loss in free enthalpy due to irreversible biochemical processes and energy conversion, it is necessary to separate the exchange of entropy between the reactor and its surroundings and an entropy production rate in the reactor.

Magnitudes of variations in stored energy functions are determined by net work, heat, and mass transfers. The basic principles of the first and second laws of thermodynamics lead to the well-known relationship between internal energy, entropy, and chemical potentials of the species, namely the Gibbs equation (Prigogine, 1967; Walas, 1985):

$$dU = T\,dS - P\,dV + \sum_i \mu_i \, dn_i \tag{11}$$

Considering an isochoric system, this relation can be rewritten as follows:

$$\frac{du}{dt} = T\frac{ds}{dt} + \sum_i \mu_i \frac{dC_i}{dt} \tag{12}$$

The macroscopic mass and internal energy balances are then considered in order to express the rate of accumulation of entropy ds/dt. The partial molar entropies of the species must be calculated accounting for the entropies of mixing in the different flows, in and out of the reactor. This leads to (from Eqs. 5, 6, 8, and 12):

$$T\frac{ds}{dt} = \Phi_q + T\sum_i \Phi_i s_i + \Phi_w - \frac{1}{V}\int_V \nabla \cdot \int_0^\infty F_\lambda \, d\lambda \, dV - \sum_i q_i \mu_i \tag{13}$$

where Ts_i is the difference between the enthalpy of i and the chemical potential of i, that is, the partial molar entropy of i in the incoming and outgoing flows.

The rate of entropy accumulation in the system is further split into a flow of entropy through the system and a rate of entropy production. The latter accounts for all the irreversibilities produced in the system; the second law of thermodynamics states that this entropy production rate must exceed zero. This macroscopic entropy balance can then be rewritten as the addition of two terms involving entropy production q_s, and entropy convection, Φ_s:

$$T\frac{ds}{dt} = Tq_s + T\Phi_s \tag{14}$$

At thermodynamic equilibrium (nonreacting, nonstirred, nonlight energy consuming system), the entropy production must be equal to zero; this allows Φ_s and q_s to be identified separately (Glansdorff and Prigogine, 1971; Roels, 1983; Dussap, 1988):

$$\Phi_s = \frac{\Phi_q}{T} + \sum_i \Phi_i s_i \tag{15}$$

$$q_s = \frac{\Phi_w}{T} - \frac{1}{VT}\int_V \nabla \cdot \int_0^\infty F_\lambda \, d\lambda \, dV - \frac{1}{T}\sum_i q_i \mu_i \tag{16}$$

Equation 16 contains three contributions for the entropy production rate inside the reactor. The first term Φ_w/T represents the mechanical energy dissipations associated with the mechanical energy input and with the self motility of the microorganisms. To retain the entropy production rate associated with the biochemical transformations and with the light energy conversion, the mechanical energy input must be eliminated; any mechanical energy dissipated by the microorganisms themselves always represents a negligible share of total dissipation, which justifies removing the term Φ_w/T from Eq. 16. The rate of entropy production associated with the biochemical transformations and the light energy conversion is called the dissipation function $\langle\sigma\rangle$ and indicates the rate of loss (or dissipation) of free enthalpy due to irreversible processes other than stirring.

If the assumption of steady state for light energy conversion and dissipation is made and if the volumetric rate of radiant energy absorbed $\mathcal{A}$ is used, Eq. 16 is then rewritten as follows:

$$\langle\sigma\rangle = \frac{1}{T}\left[\frac{1}{V}\int_V \mathcal{A}\, dV - \sum_i q_i \mu_i\right] \tag{17}$$

The chemical affinity of the reaction j is additionally introduced; it is defined from the chemical potential and the stoichiometric coefficient matrix by:

$$A_j = -\sum_i \nu_{ij}\mu_i \tag{18}$$

This leads to the final expression of the volumetric dissipation function characterizing the chemical irreversibilities in a photoreactor:

$$\langle\sigma\rangle = \frac{1}{VT}\int_V \left[\mathfrak{A} + \sum_j J_j A_j\right] dV \tag{19}$$

For a continuous process, the steady-state assumption can be used; Eq. 14 leads to:

$$\langle\sigma\rangle = -\frac{\Phi_q}{T} - \sum_i \Phi_i s_i \tag{20}$$

which allows the quantity of heat exchanged between the system and the environment to be calculated provided the value of $\langle\sigma\rangle$ is known.

The second law of thermodynamics states that $\langle\sigma\rangle$ must be positive. Photosynthesis is a light energy driven process resulting in negative affinities for chemical conversions ($\Sigma_j \langle J_j\rangle A_j$) and a positive light energy absorption term $\langle\mathfrak{A}\rangle$.

The exergetic yield or thermodynamic efficiency is then defined by:

$$\eta_{th} = \frac{\sum_j \sum_p \nu_{pj}\langle J_j\rangle \mu_p}{\langle\mathfrak{A}\rangle - \sum_j \sum_s \nu_{sj}\langle J_j\rangle \mu_s} \tag{21}$$

where subscripts s and p refer respectively to substrates and products ($\nu_s < 0$, $\nu_p > 0$).

Also, if the arbitrary datum level for energy (reference state) has been chosen sufficiently close to the actual conditions, the chemical potentials of the different species can be considered to be equal to the reference chemical potentials μ_i^0, that is, the Gibbs energy of formation of component i. This reference state is generally considered to be a molar aqueous ideal solution, with pH = 7.

It must be stressed that Eqs. 5 to 21 relate to macroscopic balances over the photoreactor. Using a perfect mixing assumption, the state variables C_i, h_i, s_i, μ_i, and A_j remain unchanged throughout the reactor volume; the volumetric average rates $q_i = \langle r_i\rangle$, $\langle J_j\rangle$, $\langle\mathfrak{A}\rangle$ and $\langle\sigma\rangle$ are taken by averaging the local rates over the entire volume of the photoreactor. Although the average conversion rates $\langle r_i\rangle$ and $\langle J_j\rangle$ are the only observable rates, it may be important for kinetic modeling to relate the local conversion rates to the local rate of radiant energy absorbed $\mathfrak{A}$. Kinetic assumptions concerning the metabolic activities of organisms may be confidently made directly from the local dissipation function. Although no formal demonstration is made, the local dissipation function σ for a monophasic system must be given by:

$$\sigma = \frac{1}{T}\left[\mathfrak{A} + \sum_j J_j A_j\right] \tag{22}$$

Given that the dissipation function aggregates kinetic and energetic aspects, kinetic information on the quantities J_j are required with thermodynamic quantities A_j, to evaluate the chemical irreversibility term in Eq. 19. Such kinetic information is related to the volumetric rate of radiant energy absorbed by means of a conversion yield of light in species j:

$$J_j = Y_{I/j}\mathfrak{A} \tag{23}$$

The determination of the local conversion yield $Y_{I/j}$ involves a detailed description of the metabolic phenomena such as membrane diffusion processes and their coupling with electron transport, hydrogen ion transport, and photon trapping. However, such microscopic analysis of the functioning of biological membranes lies outside the scope of this article.

From the above, it is evident that the local rate of radiant energy absorbed $\mathfrak{A}$ is crucial. This must be obtained by the balance for the photonic phase.

Radiant light energy balance for the photonic phase

As previously mentioned, an additional scalar local equation is needed for the photonic phase, in order to determine the term for the radiant energy exchanged between the two phases. This local equation should have the general form of the radiative transfer equation (Spadoni et al., 1978; Aiba, 1982; Siegel and Howell, 1992), and is needed to differentiate between light absorbed and scattered by microorganisms.

The radiant energy term must be obtained from the steady-state general form of the equation of radiative transfer (Chandrasekhar, 1960; Spadoni et al., 1978; Aiba, 1982) in local specific intensity I of wavelength λ, and for direction $\boldsymbol{u}$ (Figure 1):

$$\int_0^\infty (\boldsymbol{u}\cdot\nabla) I_\lambda\, d\lambda = -\int_0^\infty [Ea(\lambda) + Es(\lambda)] C_X I_\lambda\, d\lambda + \int_0^\infty \frac{Es(\lambda)}{4\pi} C_X \int_{\Omega'} p(\boldsymbol{u},\boldsymbol{u}') I_\lambda\, d\omega'\, d\lambda \tag{24}$$

$Ea(\lambda)$ and $Es(\lambda)$ are respectively the absorption and scattering mass coefficients for wavelength λ. C_X is the biomass concentration in the photobioreactor which is directly related to absorption and scattering coefficients (Beer law extension), showing that all the radiative transfers in the photobioreactor are governed by microorganisms. The first term on the right-hand side of Eq. 24 denotes loss of radiant energy by absorption and scattering along direction $\boldsymbol{u}$, and the second term denotes gain of radiant energy scattered from all directions of space.

$p(\boldsymbol{u},\boldsymbol{u}')$ is the phase function which stands for the spatial distribution of scattered radiant energy. Generally, it can be expanded as a series in a Legendre polynomial of the form (Chandrasekhar, 1960):

$$p(\boldsymbol{u},\boldsymbol{u}') = p(\cos\Theta) = \sum_{l=0}^{\infty} \bar{\omega}_l P_l(\cos\Theta) \tag{25}$$

If the photonic phase is assumed to be isotropic, the phase function remains constant and equal to unity:

$$p(\cos\Theta) = 1 \tag{26}$$

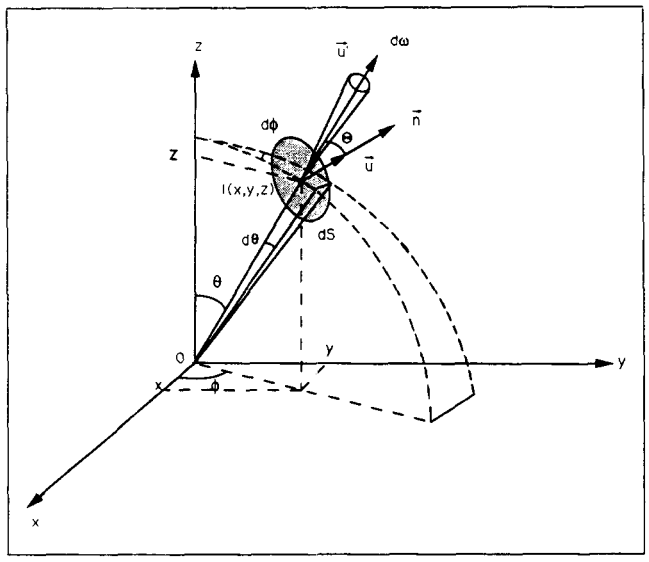

Figure 1. Definition of specific local intensity *I* in radiant light energy for direction *u*.

Integration of *I* over all directions of space from the normal n affords the definition of the radiant energy flux vector *F*. Average of *I* over all directions on 4π steradians denotes the mean specific intensity *J*.

From the definitions of the radiant energy flux F_λ and the mean specific intensity J_λ which are respectively equal to:

$$F_\lambda = \int_\Omega I_\lambda \cos\theta \, d\omega \tag{27}$$

$$J_\lambda = \frac{1}{4\pi} \int_\Omega I_\lambda \, d\omega \tag{28}$$

Eq. 24 can be integrated (Figure 1) over all directions of space and over all wavelengths in the spectrum, yielding:

$$-\int_0^\infty \nabla \cdot F_\lambda \, d\lambda = 4\pi \int_0^\infty Ea(\lambda)\, C_X J_\lambda \, d\lambda \tag{29}$$

In Eq. 27, θ is the angle from the normal n of a surface reference dS to the direction of I_λ. Since θ is in the integral, flux F_λ depends on the direction of n; hence F_λ is a vector.

Equation 29 is the same as Eq. 4 with the local volumetric rate of radiant energy absorbed defined by the following expression:

$$\mathcal{A} = \int_0^\infty \int_\Omega Ea(\lambda)\, C_X I_\lambda \, d\omega \, d\lambda = 4\pi \int_0^\infty Ea(\lambda)\, C_X J_\lambda \, d\lambda \tag{30}$$

J_λ being the mean specific intensity.

The local absorption rate of radiant energy is then determined from knowledge of the mean energy available by the microorganisms $4\pi \int_0^\infty J_\lambda \, d\lambda$. This quantity seems the most efficient variable for modeling radiative transfer phenomena in photobioreactors.

For simplified plane parallel monodimensional applications, in the z-direction, Eqs. 4 and 30 reduce to (Chandrasekhar, 1960):

$$\mathcal{A} = -\int_0^\infty \frac{\partial}{\partial z}[F_\lambda(z)]\, d\lambda = -\int_0^\infty \int_0^{2\pi} \int_{-1}^{+1} \mu \frac{dI_\lambda}{dz} \, d\mu \, d\phi \, d\lambda \tag{31}$$

with $\mu = \cos\theta$, θ being the angle with the normal vector, and ϕ being the azimuthal angle.

Hence, Eq. 24 becomes (Chandrasekhar, 1960):

$$-\mu \frac{1}{[Ea(\lambda) + Es(\lambda)]C_X} \frac{dI_\lambda}{dz} = I_\lambda - \frac{1}{2}\bar{\omega}_0 \int_{-1}^{+1} I_\lambda \, d\mu' \tag{32}$$

where $\underline{\omega}_0$ is the albedo of single scattering: $\underline{\omega}_0 = [Es(\lambda)/Ea(\lambda) + Es(\lambda)]$.

This equation has to be solved when a monodimensional approximation is made, in order to obtain the volumetric rate of radiant energy absorbed.

Analytical approximized monodimensional solution

The monodimensional form of the equation of radiative transfer (Eq. 32) may be numerically solved from two to eight flux methods (Chandrasekhar, 1960; Daniel et al., 1979; Siegel and Howell, 1992). A comparative analysis of the efficiency of 2-6 flux methods has been performed by Daniel et al. (1979) and Siegel and Howell (1992) and showed that the two flux method was sufficiently accurate as a first approximation to obtain profiles of radiant energy through a radiation field.

Thus, assuming an isotropic radiation field, Eq. 32 reduces to a system of two ordinary differential equations with a known analytical solution.

This two-flux method was proposed by Schuster (1905) and used by Cornet et al. (1992a) to model radiative transfer in parallelepiped photobioreactors.

An analytical expression in the z-profile of the local radiant energy available gives, as reported by Cornet et al. (1992a):

$$4\pi \int_\lambda J_\lambda(z)\, d\lambda = 2 \int_\lambda F_\lambda^0 \, d\lambda \, \frac{[(1+\alpha)e^{-\delta(Z-1)} - (1-\alpha)e^{\delta(Z-1)}]}{(1+\alpha)^2 e^{\delta} - (1-\alpha)^2 e^{-\delta}} \tag{33}$$

with $\alpha = [Ea/(Ea+Es)]^{1/2}$, $\delta = (Ea+Es)\ \alpha C_X L$ and Z being the dimensionless abscissa z/L.

In this equation, light is taken to be supplied only on one side of the reactor, and L represents the optical thickness of the reactor.

Note that Eq. 33 includes mean global absorption and scattering coefficients: $Ea = (1/\Delta\lambda) \int_\lambda Ea(\lambda)\, d\lambda$ and $Es = (1/\Delta\lambda) \int_\lambda Es(\lambda)\, d\lambda$.

For monodimensional approximations, $\langle \mathcal{A} \rangle$ can be defined as:

$$\langle \mathcal{A} \rangle = \frac{1}{L} \int_0^L \mathcal{A}(z)\, dz$$

and the dimensionless mean absorption rate of radiant energy is written as (Cornet et al., 1992a):

$$\frac{\langle \mathfrak{A} \rangle}{\langle \mathfrak{A}_0 \rangle} = 1 - \left[\frac{4\alpha + (1-\alpha^2)(e^{\delta} - e^{-\delta})}{(1+\alpha)^2 e^{\delta} - (1-\alpha)^2 e^{-\delta}} \right] \tag{34}$$

where $\langle \mathfrak{A}_0 \rangle$ is the volumetric rate of total incident radiant energy illuminating the reactor, that is:

$$\langle \mathfrak{A}_0 \rangle = \frac{1}{V} \int_0^{\infty} \int_S \int_{\Omega} I_{\lambda} \, d\omega \, dS \, d\lambda.$$

In addition, it is easily established that the limiting value reached by the ratio $\langle \mathfrak{A} \rangle / \langle \mathfrak{A}_0 \rangle$, as the biomass concentration increases in the reactor becomes:

$$\lim_{c_X L \to \infty} \frac{\langle \mathfrak{A} \rangle}{\langle \mathfrak{A}_0 \rangle} = \frac{2\alpha}{1+\alpha} \tag{35}$$

where α is defined in Eq. 33.

Numerical tridimensional solution

Complex problems arise in the resolution of the tridimensional form of the radiative transfer equation (Eq. 24) from:

- The radiant nature of light energy, which leads to an integro-differential equation; and
- Its application to a tridimensional finite medium for different geometries.

Generally, the Monte Carlo method is used to solve the general equation of radiative transfer (Spadoni et al., 1978; Aiba, 1982; Siegel and Howell, 1992). This is a stochastic method which has the disadvantages of poor accuracy and very high calculation time.

Thus modeling and simulation of batch cultures with this method is unsuitable because calculation of the volumetric rate of radiant energy absorbed is required at each step of the numerical integration of complex time dependent equations.

A new method using finite elements is presented here (Appendix A). It uses the explicit algorithm of the characteristic curve developed by Pironneau (1989), the convergence of which is particularly suitable for the present study.

Equation 24 must be solved for each wavelength λ in the visible spectrum. To minimize calculation time, the algorithm has accordingly been vectorized. The gain obtained depends on the discretization of λ, but the scalar calculation time may be reduced by a factor of up to 20.

Applications to Rectangular and Cylindrical Photobioreactors

Materials and methods

The photosynthetic microorganism used was the filamentous cyanobacterium *Spirulina platensis*. Strain 8005 of the Institut Pasteur was grown axenically in a modified Zarrouk medium (Cornet et al., 1992b).

Three different photobioreactors were used for these experiments:

- Two parallelepiped photobioreactors of respectively 1 and 4 L total volume (optical thickness $5 \cdot 10^{-2}$ and $8 \cdot 10^{-2}$ m, respectively);
- A cylindrical photobioreactor (Applikon) of 7 L total volume (internal diameter of 1.6 10^{-1}m).

For the parallelepiped reactors, the light was supplied by four white fluorescent lamps (20 W, Mazdafluor, white industry TF), to one side of the reactor. The other sides were covered with black paper.

For the cylindrical reactor, the light was supplied to half of the total annular area by two halogen lamps (500 W, Philips, R7S). The opposite half and the bottom of the reactor were covered with black paper.

The absorption and scattering mass coefficients for each wavelength were determined spectrophotometrically, according to Aiba (1982), and Shibata (1958).

The mean absorption and scattering coefficients were obtained respectively by the following integrals on the visible spectrum (in nanometers):

$$Ea = \frac{1}{\Delta\lambda} \int_{350}^{750} Ea(\lambda) \, d\lambda, \; Es = \frac{1}{\Delta\lambda} \int_{350}^{750} Es(\lambda) \, d\lambda.$$

The experimental determinations of the mean volumetric rate of radiant energy absorbed in parallelepiped reactors were obtained from the opalescent plate method described by Aiba (1982).

The biomass reaction rates $\langle J_X \rangle$ were obtained on the three photobioreactors with different incident light fluxes during batch and continuous cultures. For batch cultures, $\langle J_X \rangle$ was taken as the linear volumetric growth rate of biomass; importantly, biomass concentration was always high enough (>1 kg/m^3) to ensure that the mean volumetric rate of radiant energy absorbed $\langle \mathfrak{A} \rangle$ was maximum. For continuous cultures, $\langle J_X \rangle$ was taken as the biomass productivity obtained in the reactor.

All the numerical calculations were performed on a Siemens VP 200 vectorial supercomputer.

Results and Discussion

Volumetric rate of radiant energy absorbed

Figure 2 shows 40 values obtained for the absorption and scattering mass coefficients in the visible spectrum. The scattering mass coefficient is independent of wavelength in the range 350–750 nm because of the large size of the filamentous microorganisms (100–250 μm) compared to visible wavelengths. This remains true at all stages after inoculation because the cultures are not synchronized and the cyanobacteria considered are pluricellular microorganisms. On the contrary, for unicellular microorganisms (0.5–3 μm), a dependency of the scattering mass coefficient on the wavelength would occur in the visible spectrum.

The main photosynthetic pigments, chlorophyll *a* and phycocyanin, are responsible for the values of the absorption coefficient, the evolution of which is similar to the absorption spectrum for the microorganisms concerned.

Figure 3 shows 40 values of the albedo of single scattering in the visible spectrum. The high values obtained (between 0.45 and 0.90), show that the scattering mass coefficient can never be neglected compared with the absorption mass coefficient. This is a justification for the choice of the radiative transfer

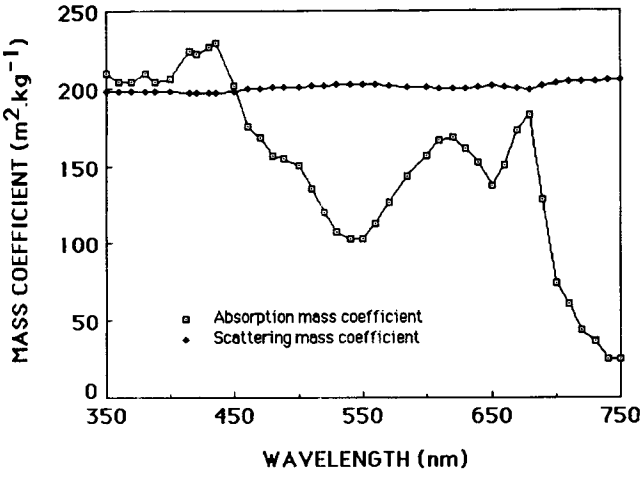

Figure 2. Absorption and scattering mass coefficients for each wavelength in the range of visible spectrum.

theory to describe the photonic phase in photobioreactors, rather than Lambert's theory (Spadoni et al., 1978; Daniel et al., 1979; Aiba, 1982).

From these results, the values obtained for the mean absorption and scattering coefficients are the following:

$$Ea = 150 \text{ m}^2 \cdot \text{kg}^{-1}$$

$$Es = 200 \text{ m}^2 \cdot \text{kg}^{-1}$$

These mean coefficients allow the analytical calculation of the normalized ratio $\langle \mathcal{A} \rangle / \langle \mathcal{A}_0 \rangle$ for parallelepiped reactors, that is, the volumetric rate of radiant energy absorbed divided by the potential maximum volumetric rate of radiant incident energy.

Experimental determinations of the ratio $\langle \mathcal{A} \rangle / \langle \mathcal{A}_0 \rangle$ for the two parallelepiped reactors and for an incident homogeneous flux of 40 W/m^2 (fluorescent lamps) vs. the biomass concentration are plotted on Figure 4. The solid and dotted lines represent the results of the analytical solution provided by Eq. 34, at two different optical thicknesses. The asymptotic value

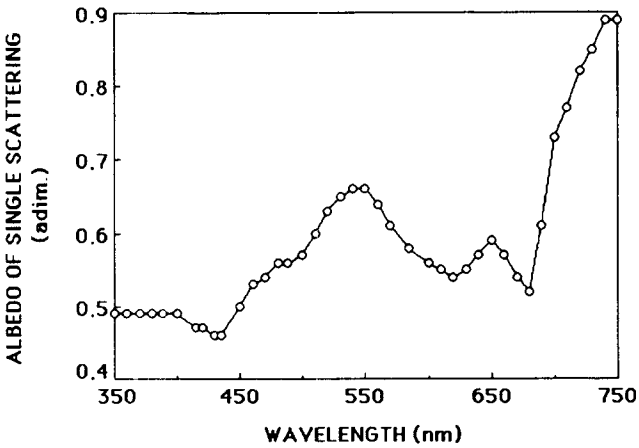

Figure 3. Albedo of single scattering $\bar{\omega}_0$ in the range of visible spectrum.

Calculation is done from the isotropic field of radiation hypothesis.

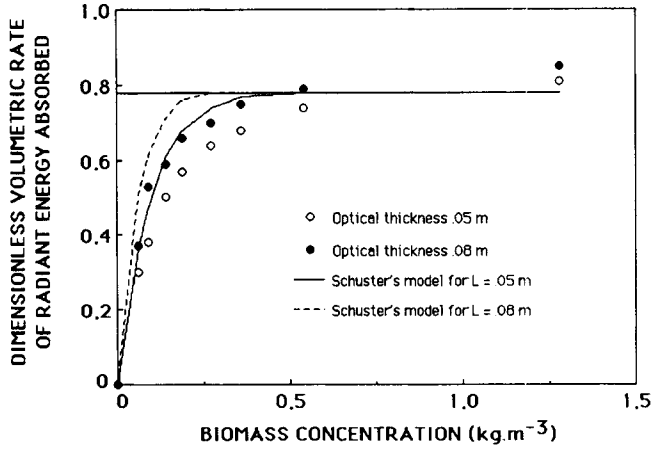

Figure 4. Calculated vs. experimental values of the dimensionless volumetric rate of energy absorbed vs. biomass concentration.

Results were obtained from two rectangular photobioreactors of optical thicknesses 0.05 and 0.08 m, respectively. Solid and dotted lines stand for the analytical approximated monodimensional solution for the volumetric rate of radiant energy absorbed (Eq. 34). Asymptotic value for the ratio $\langle \mathcal{A} \rangle / \langle \mathcal{A}_0 \rangle$ given by Eq. 35 is also presented.

of the ratio $\langle \mathcal{A} \rangle / \langle \mathcal{A}_0 \rangle$ calculated by Eq. 35 for high biomass concentration is added. For the microorganisms concerned, the α parameter is equal to 0.655 and Eq. 35 gives a maximum value for this ratio of 0.79.

Equation 35 thus provides a fair approximation for the ratio $\langle \mathcal{A} \rangle / \langle \mathcal{A}_0 \rangle$, when the biomass concentration is high. However, an analytical solution of Eq. 34 does not seem sufficiently accurate to describe the evolution of the volumetric rate of radiant energy absorbed for biomass concentrations down to 1 kg/m^3. For high biomass concentration only a fraction of the reactor is illuminated because of the absorption of radiant light energy by high pigment density. This part of the reactor defines an illuminated working volume in which only growth occurs (Cornet et al., 1992a,b). As the illuminated working volume decreases, the loss of scattered radiation from the reactor in the two dimensions of space neglected also decreases and approaches zero. In this case, for high biomass concentration (>1 kg/m^3), the monodimensional approximation is fully justified as observed in Figure 4. Conversely, for low biomass concentration, a large part of the total incident energy is scattered from the total volume of the reactor and the monodimensional approximation is inadequate.

In Figure 5, the same experimental results are shown, but here the solid and dotted lines have been obtained by numerical calculation from the gridding algorithm presented in Appendix A. It must be emphasized that the model requires two experimental parameters $Ea(\lambda)$ and $Es(\lambda)$ which are measured independently (Shibata, 1958; Aiba, 1982). Experimental values and numerical calculations are in fairly good agreement, irrespective of the biomass concentration or the optical thickness in the photoreactor.

Figure 6 shows the results of a numerical calculation of the ratio $\langle \mathcal{A} \rangle / \langle \mathcal{A}_0 \rangle$ vs. the biomass concentration for a cylindrical reactor. The incident homogeneous flux was 40 W/m^2 and was supplied by halogen lamps. This ratio reaches an asymptotic value at about 0.6 for the same biomass concentration as in

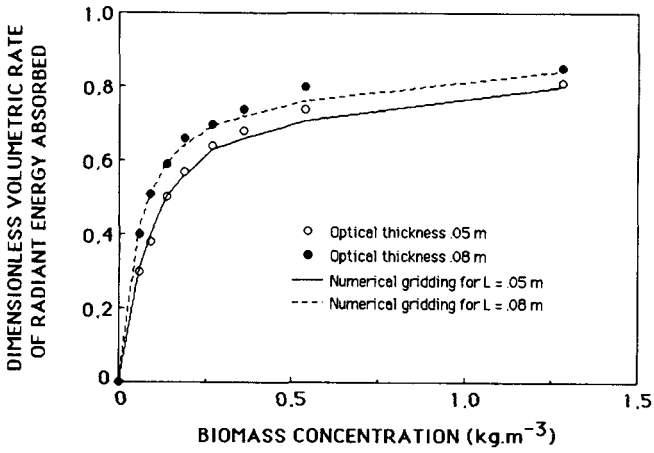

Figure 5. Calculated vs. experimental values of the dimensionless volumetric rate of energy absorbed vs. biomass concentration.

Results were obtained from two rectangular photobioreactors of optical thicknesses 0.05 and 0.08 m, respectively. Solid and dotted lines stand for the numerical tridimensional gridding for the determination of the volumetric rate of radiant energy absorbed by the algorithm presented in Appendix A. (Resolution of the general form of the equation of radiative transfer: Eq. 24.)

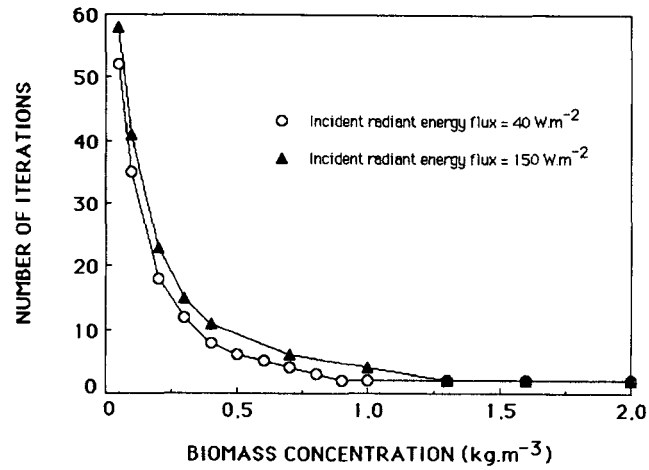

Figure 7. Convergence rate of the numerical algorithm presented in Appendix A vs. biomass concentration in the reactor.

Number of iterations to reach the convergence is determined for two different incident radiant energy fluxes of 40 and 150 W·m^{-2}, respectively.

the parallelepiped reactor. This means that a greater proportion of the incident energy was scattered from the cylindrical reactor than from the parallelepiped reactor illuminated on one side.

In addition, there is a difference of up to 20% between the calculation with global coefficients and the calculation with coefficients for each wavelength. This indicates that it is more accurate to use the absorption and scattering coefficients for each wavelength instead of mean absorption and scattering coefficients, when the emission spectrum of the lamps displays changes in energy distribution with wavelength, in order to compute the energy balance for each radiation. This is particularly important for the halogen lamps used for illuminating the cylindrical photobioreactor which provide most of the energy in the red range.

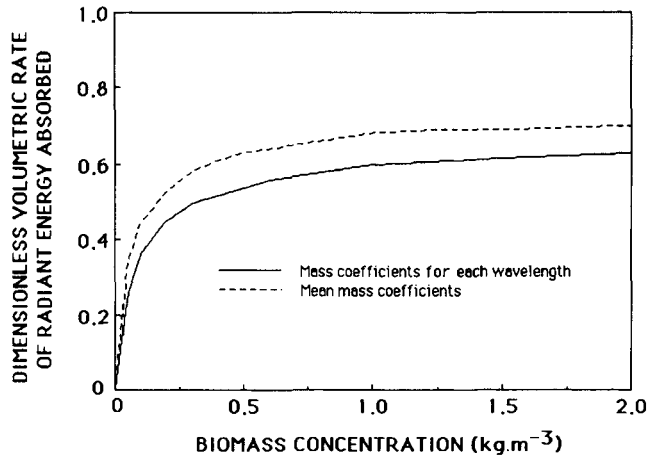

Figure 6. Numerical tridimensional calculation of the dimensionless volumetric rate of radiant energy absorbed vs. biomass concentration for a cylindrical photobioreactor.

Comparison between the utilization of absorption and scattering mass coefficients for each wavelength (solid line), and mean global mass coefficients (dotted line).

In Figure 7 the convergence of the numerical algorithm is rapidly increased as the biomass concentration increases in the reactor. From a concentration of 1 kg/m^3, the convergence is obtained with a minimum number of iterations of 2. This must be related to the decrease in the illuminated working volume, as other parts of the reactor remain dark and inoperative.

The results described show that the numerical gridding of photobioreactors in specific intensity (Eq. 24), is the most suitable and most accurate way to obtain the mean local intensity available by microorganisms $4\pi \int_0^\infty J_\lambda d\lambda$, and also the volumetric rate of radiant energy absorbed in the reactor.

The method and the algorithm presented in this article allow local and macroscopic information on radiant energy available in general tridimensional geometries to be calculated. This is a basic requirement for energy balances to study the conversion of radiant energy into chemical affinity.

This information is also necessary to establish kinetic laws and determine the chemical reaction term in microorganisms, since in photobioreactors the radiant light energy is a limiting factor for growth kinetics.

On the other hand, the monodimensional approximation, based on the assumptions of Schuster (1905), seems limited to the prediction of asymptotic determination for the ratio $\langle \mathcal{A} \rangle / \langle \mathcal{A}_0 \rangle$, when the biomass concentration is high. For low biomass concentrations, the lack of consideration of light scattering in the reactor in two dimensions of space is essentially responsible for the differences observed between experimental and analytical values (Eq. 34). Also, this approach is restricted to simplified geometries such as parallelepiped reactors or cylindrical reactors with a radial incident light intensity, and requires the flux of incident light to be homogeneous over the total entry area.

Thus, the monodimensional simplification is fundamentally flawed; the experimental apparatus has to be adapted to allow for the theoretical approximations of the model.

Table 1 Experimentally Determined Biomass Reaction Rates; Dissipation Function of Entropy and Thermodynamic Photosynthesis Efficiency for Different Volumetric Rates of Radiant Energy Absorbed

Mean Vol Rate of Radiant Energy Abs. $\langle \mathcal{A} \rangle$ ($W \cdot m^{-3}$)	Reaction Rate $\langle J_X \rangle$ ($kmol \cdot m^{-3} \cdot s^{-1}$)	$-\sum \langle J_X \rangle \cdot A_j$ ($W \cdot m^{-3}$)	Dissipation Function of Entropy $\langle \sigma \rangle$ ($W \cdot m^{-3} \cdot K^{-1}$)	Thermodyn. Efficiency ηth
80*	1.95×10^{-8}	12.1	0.22	0.15
110*	2.46×10^{-8}	15.2	0.31	0.14
140*	3.02×10^{-8}	18.7	0.39	0.13
180*	3.78×10^{-8}	23.4	0.51	0.13
330*	5.52×10^{-8}	34.2	0.96	0.10
390*	5.95×10^{-8}	36.9	1.14	0.09
480*	6.33×10^{-8}	39.5	1.43	0.08
700*	8.50×10^{-8}	52.7	2.10	0.08
750*	8.50×10^{-8}	52.7	2.26	0.07
790**	9.67×10^{-8}	59.9	2.36	0.07
980*	1.10×10^{-7}	68.2	2.95	0.07
1,150*	1.32×10^{-7}	81.8	3.46	0.07
1,280**	1.42×10^{-7}	88.0	3.86	0.06
1,680**	1.47×10^{-7}	91.1	5.14	0.05

*(Values of $\langle \mathcal{A} \rangle$ were obtained by numerical determinations from the algorithm presented in Appendix A); *batch cultures; **continuous cultures.

Calculation of the entropy dissipation function and the thermodynamic efficiency of photosynthesis

As mentioned, the calculation of the entropy dissipation function requires prior knowledge of both a stoichiometric equation and a volumetric rate for biomass growth, in order to assess the chemical reaction term. From several batch and continuous cultures, in different photobioreactors and with different incident illuminations, the following stoichiometric equation was obtained for the growth of *Spirulina platensis* (Cornet et al., 1992b):

$$HCO_3^- + 0.69\ H_2O + 0.17NO_3^- + 0.007SO_4^{2-} + 0.184H^+ \xrightarrow{\langle J_x \rangle} CH_{1.58}O_{0.46}N_{0.17}S_{0.007} + 1.38O_2 + OH^-$$

For each incident light energy, the experimental volumetric rates of growth are reported in Table 1. In this table, the volumetric rates of radiant energy absorbed have been calculated from the numerical algorithm presented in Appendix A.

The standard free enthalpies used for the calculation of the dissipation function of entropy are defined at a pH of 7 for HCO_3^- and liquid water, and unit molality for all other reactants, a temperature of 308 K, and atmospheric pressure. These data for biomass and other species are provided by Roels (1983). The biomass standard chemical potential has been taken as $6.1\ 10^8\ J \cdot kmol^{-1}$ (Roels, 1983).

Table 1 displays the results for the dissipation function of entropy over a wide range of volumetric rate of energy absorbed for both batch and continuous cultures. Unlike aerobic processes, the chemical reaction term has a negative value. However, the dissipation function is always positive, because of the positive value of the radiant energy term at a higher level of free chemical potential, consistent with the second law of thermodynamics.

Also, the thermodynamic efficiency decreases as the volumetric rate of radiant energy absorbed increases in the reactor. This decrease is correlated with modifications in the preliminary stages of photosynthesis and particularly in electron transfer efficiency, which is dramatically impaired by a high flux of photons. The highest value of 0.15 in exergetic yield was found for low volumetric rates of radiant energy, that is, for low light energy inputs. In these cases, the values obtained for the mean radiant energy available in the reactor $\int_0^\infty 4\pi J_\lambda\, d\lambda$ are less than $10\ W \cdot m^{-2}$, which corresponds to the maximum quantum yield for photosynthesis.

It must be emphasized that the general behavior of the thermodynamic efficiency can be represented as the sole function of the volumetric rate of radiant energy absorbed whether batch or continuous cultures are concerned. This clearly indicates that the partition of the entropy balance between an entropy production term (dissipation) and an entropy convective term has been properly made. Furthermore, the dissipation function appears to be a key variable for correlating the conversion yield of light energy into chemical affinity.

These results show that thermodynamic efficiency must be defined from energy balances and from the entropy dissipation function rather than from the enthalpy balance as many authors have suggested (Aiba and Ogawa, 1977; Ogawa and Aiba, 1978; Ogawa et al., 1978; Lee and Pirt, 1982; Aiba and Ogawa, 1983; Lee et al., 1984, Iehana, 1987; Lee et al., 1987). In addition, the fraction of the dissipated energy corresponding to the maintenance of the microorganisms can be determined from experiments performed in different conditions of volumetric rate of radiant energy absorbed if the local energy profiles are calculated. This affords a correlation of the quantum yield (Eq. 23) from a detailed description of the metabolic pathways that ensure the conversion of radiant energy (Roels, 1983; Dussap, 1988).

Conclusion

In this article, the expression of the entropy dissipation function for light energy absorption and biochemical conversions has been theoretically established from energy and mass balances on an isothermal, absorbing, and scattering medium characterizing a photobioreactor. The dissipation function provides a measure of the energy problems arising in the con-

version of radiant light energy into chemical affinity by photosynthetic microorganisms.

In addition, this approach allows a definition of the thermodynamic efficiency of photosynthesis in photobioreactors. The dissipation function aggregates all the irreversibilities in the system and exhibits a negative affinity term and a positive rate of radiant energy absorbed. This causes calculation difficulties because of the radiant nature of light and the nonanisotropy of the medium in light distribution. Accordingly, the local equation of radiative transfer has to be solved to determine this volumetric rate of radiant energy absorbed.

This absorption rate determination is shown to be the preliminary step for the calculation of the dissipation function. It also enables assessment of growth kinetics in biomass, as the light energy consumption by microorganisms is the rate limiting process for photosynthesis, if a conversion yield of light in biomass is introduced.

Two different methods for calculating the absorption rate of radiant energy in photobioreactors are presented in this article. A complex tridimensional and a new numerical method using finite elements are compared with an analytical monodimensional approximized method. The ability of the monodimensional approximations is shown to be restricted to high biomass concentrations.

From experimental results with the cyanobacterium *Spirulina platensis* and numerical determinations of $\langle \mathfrak{A} \rangle$, the dissipation function has been calculated for different conditions of light energy inputs and for different reactor geometries. This allows an assessment of the thermodynamic efficiency of photosynthesis. This exergetic yield is shown to reach the peak value of 15% when the absorption rate of radiant energy is low, that is, when the mean quantum yield is maximum in the photobioreactor.

In addition, knowledge of local radiant light absorption rate may allow the calculation of the local quantum yield.

Acknowledgments

The authors are grateful to the European Space Agency (ESA), and the Centre National d'Etudes Spatiales (CNES) for their financial support through the MELiSSA project of ESA.

We thank J. M. Teuler of the Centre Inter Regional de Calcul Electronique (CIRCE Orsay) and Y. Maday of the Laboratoire d'Analyse Numérique of the University of Paris VI (Jussieu) for their helpful advice and technical support.

All the experimental determinations were performed at the CNRS Laboratoire de Biochimie Fonctionnelle des Membranes Végétales (Gif sur Yvette). We are especially indebted to G. Dubertret and A. Tremolieres.

Notation

$\mathfrak{A}$ = local volumetric rate of radiant energy absorbed, $W \cdot m^{-3}$
A_j = affinity of compound j, $J \cdot kmol^{-1}$
C_i = concentration of compound i, $kmol \cdot m^{-3}$
C_X = concentration of biomass, $kg \cdot m^{-3}$
Ea = mean absorption mass coefficient, $m^2 \cdot kg^{-1}$
$Ea(\lambda)$ = absorption mass coefficient relative to wavelength λ, $m^2 \cdot kg^{-1}$
Es = mean scattering mass coefficient, $m^2 \cdot kg^{-1}$
$Es(\lambda)$ = scattering mass coefficient relative to wavelength λ, $m^2 \cdot kg^{-1}$
F = mean flux of radiant energy, $W \cdot m^{-2}$
F_λ = flux of radiant energy for wavelength λ, $W \cdot m^{-3}$
h_i = partial molar enthalpy, $J \cdot kmol^{-1}$
I = mean specific intensity, $W \cdot m^{-2}$
I_λ = specific intensity for wavelength λ, $W \cdot m^{-3}$
J = mean intensity for total spectrum, $W \cdot m^{-2}$
J_j = rate of reaction j, $kmol \cdot m^{-3} \cdot s^{-1}$
J_λ = mean intensity for wavelength λ, $W \cdot m^{-3}$
L = total length of reactor, m
n_i = molar fraction for compound i, dimensionless
N_i = molar flux of compound i, $kmol \cdot m^{-2} \cdot s^{-1}$
$p(u,u')$ = phase function, dimensionless
P = pressure, Pa
q = flux of heat conduction, $W \cdot m^{-2}$
q_i = mean volumetric reaction rate, $kmol \cdot m^{-3} \cdot s^{-1}$
q_s = entropy production rate, $W \cdot m^{-3} \cdot K^{-1}$
r_i = local volumetric reaction rate, $kmol \cdot m^{-3} \cdot s^{-1}$
s = volumetric entropy $J \cdot m^{-3} \cdot K^{-1}$
s_i = specific entropy for compound i, $J \cdot kmol^{-1} \cdot K^{-1}$
S = entropy, $J \cdot K^{-1}$
t = time, s
T = temperature, K
u = unit vector, dimensionless
u = volumetric internal energy, $J \cdot m^{-3}$
U = internal energy, J
v = velocity, $m \cdot s^{-1}$
V = volume, m^3
$Y_{I/j}$ = conversion yield of light in species j, $kmol \cdot J^{-1}$
z = length, m
Z = dimensionless length, dimensionless
$\langle\ \rangle$ = $1/V \int_V \cdot dV$, mean volumetric integral

Greek letters

α = $[Ea/(Ea+Es)]^{1/2}$, dimensionless
δ = $(Ea+Es)\alpha C_X L$, dimensionless
η = dynamic viscosity, Pa·s
η_{th} = thermodynamic efficiency, dimensionless
θ = angle, rd
Θ = angle, rd
λ = wavelength, m
λ_T = heat conductivity, $W \cdot m^{-1} \cdot K^{-1}$
μ_i = chemical potential for compound i, $J \cdot kmol^{-1}$
μ_i^0 = standard chemical potential for compound i, $J \cdot kmol^{-1}$
ν_{ij} = stoichiometric coefficient, dimensionless
σ = entropy dissipation function, $W \cdot m^{-3} \cdot K^{-1}$
τ = stress tensor, Pa
ϕ = angle, rd
Φ = viscous dissipation function, s^{-2}
Φ_i = molar flow rate for compound i, $kmol \cdot m^{-3} \cdot s^{-1}$
Φ_q = caloric power, $W \cdot m^{-3}$
Φ_S = flow rate of entropy, $W \cdot m^{-3} \cdot K^{-1}$
Φ_W = work power, $W \cdot m^{-3}$
Ω, Ω' = solid angle, dimensionless
ω, ω' = solid angle, dimensionless
$\overline{\omega}_0$ = albedo of single scattering, dimensionless

Literature Cited

Aiba, S., "Growth Kinetics of Photosynthetic Microorganisms, *Biochem. Eng.*, **23**, 85 (1982).

Aiba, S., and T. Ogawa, "Assessment of Growth Yield of a Blue Green Algae, *Spirulina platensis*, in Axenic and Continuous Cultures," *J. Gen. Microbiol.*, **102**, 179 (1977).

Aiba, S., and T. Ogawa, "On the Criticism of Some Measurements of Photosynthetic Efficiency," *Biotech. Bioeng.*, **25**, 2775 (1983).

Bird, R. B., W. E. Stewart, and E. N. Lightfoot, *Transport Phenomena.*, John Wiley, New York (1960).

Chandrasekhar, S., *Radiative Transfer*, Dover Publications Inc., New York (1960).

Cornet, J. F., C. G. Dussap, and G. Dubertret, "Structured Model for Simulation of Cultures of the Cyanobacterium *Spirulina platensis* in Photobioreactors. I. Coupling between Light Transfer and Growth Kinetics," *Biotech. Bioeng.*, **40**, 817 (1992a).

Cornet, J. F., C. G. Dussap, P. Cluzel, and G. Dubertret, "Structured Model for Simulation of Cultures of the Cyanobacterium *Spirulina platensis* in Photobioreactors. II. Identification of Kinetic Parameters Under Light and Mineral Limitations," *Biotech. Bioeng.*, **40**, 826 (1992b).

Daniel, K. J., N. M. Laurendeau, and F. P. Incropera, "Predictions of Radiation Absorption and Scattering in Turbid Water Bodies," *ASME J. Heat Transfer*, **101**, 63 (1979).
Doelle, H. W., *Bacterial Metabolism*, 2nd ed., Academic Press, London (1975).
Dussap, C. G., "Etude Thermodynamique et Cinétique de la Production de Polysaccharides Microbiens par Fermentation en Limitation par le Transfert d'Oxygène. Modèle Structuré de la Production de Xanthane," Thèse de Doctorat ès Sciences Physiques, Université B. Pascal, Clermont-Ferrand, France (1988).
Glansdorff, P., and I. Prigogine, *Thermodynamic Theory of Structure, Stability and Fluctuations*, John Wiley Intersciences, London (1971).
Iehana, M., "Kinetic Analysis of the Growth of *Spirulina sp.* in Batch Culture," *J. Ferment. Technol.*, **65**, 267 (1987).
Lee, Y. K., L. E. Erickson, and S. S. Yang, "The Estimation of Growth Yield and Maintenance Parameters for Photoautotrophic Growth," *Biotech. Bioeng.*, **26**, 926 (1984).
Lee, Y. K., L. E. Erickson, and S. S. Yang, "Kinetics and Bioenergetics of Light-Limited Photoautotrophic Growth of *Spirulina platensis*," *Biotech. Bioeng.*, **29**, 832 (1987).
Lee, Y. K., and S. J. Pirt, "Maximum Photosynthetic Efficiency of Biomass Growth: a Criticism of Some Measurements," *Biotech. Bioeng.*, **24**, 507 (1982).
Ogawa, T., and S. Aiba, "CO_2 Assimilation and Growth of a Blue Green Algae, *Spirulina platensis*, in Continuous Culture," *J. Appl. Chem. Biotechnol.*, **28**, 515 (1978).
Ogawa, T., T. Fujii, and S. Aiba, "Growth Yield of Microalgae: Reassessment of Y_{kcal}," *Biotech. Bioeng.*, **20**, 1493 (1978).
Pironneau, O., *Finite Element Methods for Fluids*, John Wiley, (1989).
Prigogine, I., *Introduction to Thermodynamics of Irreversible Processes*, 3rd ed., Interscience Publishers (Wiley), New York (1967).
Roels, J. A., *Energetics and Kinetics in Biotechnology*, Elsevier Biomedical Press, Amsterdam (1983).
Schuster, A., "Radiation through a Foggy Atmosphere," *Astrophys. J.*, **21**, 1 (1905).
Siegel, R., and J. R. Howell, *Thermal Radiation Heat Transfer*, 3rd ed., Hemisphere Publishing Corp. (McGraw-Hill), New York (1992).
Spadoni, G., E. Bandini, and F. Santarelli, "Scattering Effects in Photosensitized Reactions," *Chem. Eng. Sci.*, **33**, 517 (1978).
Walas, S. M., *Phase Equilibria in Chemical Engineering*, Butterworth Publishers, Boston (1985).

Appendix A: Resolution of the Tridimensional Form of the Equation of Radiative Transfer

The equation of radiative transfer in steady-state conditions for the wavelength λ is obtained from Eq. 24:

$$(\boldsymbol{u}\cdot\nabla)I(E,\boldsymbol{u},\lambda) = -[Ea(\lambda)+Es(\lambda)]C_X I(E,\boldsymbol{u},\lambda) + Es(\lambda)C_X\frac{1}{4\pi}\int\int_{4\pi} I(E,\boldsymbol{u}',\lambda)d^2\omega' \quad \text{(A1)}$$

$\boldsymbol{u}$ is a unit vector, so $|\boldsymbol{u}|=1$.

$$\boldsymbol{u} = \begin{vmatrix}\sin\theta\cos\phi\\ \sin\theta\sin\phi \quad \theta\in[0,\pi] \text{ and } \phi\in[0,2\pi]\\ \cos\theta\end{vmatrix}$$

Angular discretization

The number n of intervals taken by θ and ϕ may be chosen from a compromise between two inconsistent conditions:

- the value of n must be high enough to avoid oscillations of fluxes;
- the value of n must be low enough to minimize the calculation time.

A good value of n has been taken to eight.

Let $u_{ij}=u(\theta_i,\phi_j)$, so we have $2n(n+1)$ values of $\boldsymbol{u}$. The integral term is then discretized as follows:

$$\int\int_{4\pi} I(E,\boldsymbol{u}',\lambda)d^2\omega' = \int_{\theta=0}^{\pi}\int_{\phi=0}^{2\pi} I(E,\boldsymbol{u}(\theta,\phi),\lambda)\sin\theta\,d\theta\,d\phi \simeq \left(\frac{\pi}{n}\right)^2\sum_{i=0}^{n}\sin\theta_i\sum_{j=0}^{2n-1} I(E,\boldsymbol{u}_{ij},\lambda) = \left(\frac{\pi}{n}\right)^2\sum_{i=0}^{n}\sum_{j=0}^{2n-1}\sin\theta_i I(E,\boldsymbol{u}_{ij},\lambda) \quad \text{(A2)}$$

Spatial-temporal discretization

The application to the operator $(\boldsymbol{u}\cdot\nabla)\,I(E,\boldsymbol{u},\lambda)$ of classical finite-element methods is inefficient because it leads to very high dimension matrices.

An explicit scheme may be applied. The equation of radiative transfer is expressed in nonstationary terms, in order to search for the steady-state solution by numerical convergence:

$$\left(\frac{\partial}{\partial t}+\boldsymbol{u}\cdot\nabla\right)I(E,\boldsymbol{u},\lambda)+C_1 I(E,\boldsymbol{u},\lambda) = C_2\int\int_{4\pi} I(E,\boldsymbol{u},\lambda)d^2\omega' \quad \text{(A3)}$$

with

$$C_1 = [Ea(\lambda)+Es(\lambda)]C_X$$

$$C_2 = Es(\lambda)C_X\frac{1}{4\pi}$$

The characteristic curve method (Pironneau, 1989) was used to solve Eq. A3, observing that $(\partial/\partial t+\boldsymbol{u}\cdot\nabla)$ is the substantial derivative operator, that is, the derivative along the characteristic curve. This numerical gridding technique for the calculation of a vertex E^{n+1} leads to the following approximation:

$$\left(\frac{\partial}{\partial t}+\boldsymbol{u}\cdot\nabla\right)I(E^{n+1},\boldsymbol{u},\lambda)\simeq\frac{I(E^{n+1},\boldsymbol{u},\lambda)-I(E^n,\boldsymbol{u},\lambda)}{\Delta t} \quad \text{(A4)}$$

The position of the vertex E^{n+1} inside the domain is determined by:

$$E^{n+1}=E^n+\Delta t\boldsymbol{u} \text{ or, } E^n=E^{n+1}-\Delta t\boldsymbol{u} \quad \text{(A5)}$$

The node E^n does not belong to the gridding because Δt is lower than the smallest gridding step.

Values of $I(E^n,\boldsymbol{u},\lambda)$ are interpolated from the neighboring vertices of the previous iteration.

From the two discretizations, we have:

$$\frac{I_{ij}(E^{n+1},\lambda)-I_{ij}(E^n,\lambda)}{\Delta t}+C_1 I_{ij}(E^{n+1},\lambda) = C_2\frac{\pi^2}{n^2}\sum_{p=0}^{n}\sum_{q=0}^{2n-1}\sin\theta_p I_{pq}(E^n,\lambda) \quad \text{(A6)}$$

with

$$I_{ij}(E,\lambda)=I(E,u(\theta_i,\phi_j),\lambda)\quad\begin{vmatrix}i=0,\ldots,n\\ j=0,\ldots,2n-1\end{vmatrix}$$

$$I_{ij}(E^{n+1},\lambda)=\frac{1}{1+C_1\Delta t}\times\left[I_{ij}(E^n,\lambda)+C_2\frac{\pi^2}{n^2}\Delta t\sum_{p=0}^{n}\sum_{q=0}^{2n-1}\sin\theta_p I_{pq}(E^n,\lambda)\right]\quad\text{(A7)}$$

Observing that $\sin\theta=\sin\pi=0$, with $n=8$, we obtain:

$$I_{ij}(E^{n+1},\lambda)\frac{1}{1+C_1\Delta t}\times\left[I_{ij}(E^n,\lambda)+C_2\frac{\pi^2}{n^2}\Delta t\sum_{p=1}^{7}\sum_{q=0}^{15}\sin\theta_p I_{pq}(E^n,\lambda)\right]\quad\text{(A8)}$$

with

$$\begin{vmatrix}i=0,\ldots,8\\ j=0,\ldots,15\end{vmatrix}$$

This numerical gridding in specific intensity I, leads to the determination of the local volumetric rate of radiant energy absorbed for the vertex k, by the following double integral:

$$\mathcal{A}(k)=Ea(\lambda)C_X\left(\frac{\pi}{n}\right)^2\sum_{i=1}^{n-1}\sin\frac{i\pi}{n}\sum_{i=1}^{2n}I(k,u_{ij})\quad\text{(A9)}$$

which is the main variable involved in the calculation of the dissipation function of entropy as it has been presented in the first part of this article.

The mean volumetric rate of radiant light absorbed and the ratio $\langle\mathcal{A}\rangle/\langle\mathcal{A}_0\rangle$ are then easily obtained by summation of all the vertices inside the domain.

Manuscript received Feb. 16, 1993,, and revision received July 19, 1993.